JOURNAL OF COMPUTATIONAL PHYSICS 119, 26–33 (1995)

An Accurate Split Step Scheme for Viscous Incompressible Fluid Flow

S. J. JACOBS*

Department of Atmospheric, Oceanic, and Space Sciences, The University of Michigan, Ann Arbor, Michigan 48109-2143

Received March 19, 1993; revised September 23, 1994

The conceptual basis underlying pressure splitting schemes in fluid mechanics is clarified by deriving a split step scheme using a rational approximation procedure, and it is shown that a modified version of the method provides accurate solutions for both the velocity and the pressure. In the most effective of the algorithms proposed here the velocity is advanced in time using a variant of a current split step scheme, and the pressure is corrected by solving an additional Poisson equation ad libitum. The method is demonstrated for a sample problem. © 1995 Academic Press, Inc.

1. INTRODUCTION

Split step methods are approximations in which the solution of an evolution equation is advanced in time by solving a set of simple problems, each of which brings in a different aspect of physics. One of the most widely used methods, first investigated by Chorin [1], provides a numerical solution of the equations governing incompressible fluid flow by treating the pressure and viscous forces separately and sequentially. The aim of most recent studies of pressure splitting schemes in fluid mechanics is to improve Chorin's algorithm by devising a method that provides second or higher order temporal accuracy in the computation of the velocity.

Recently, several papers [2–4] have appeared on pressure splitting methods which remove some of the mystery from the subject. In the first of these studies, Van Kan provides a rigorous analysis of a split step method that bypasses the issue of boundary conditions on the pressure by a priori spatial discretization of the Navier–Stokes equations. In the second, Bell *et al.* make the very original observation that pressure splitting schemes consist of taking one step in an iterative procedure for advancing the solution from time t to time $t + \Delta t$, and they develop such a scheme on this basis. In the third, Dukowicz and Dvinsky derive a pressure splitting method equivalent to Van Kan's by giving an approximate solution of the system of linear equations treated iteratively by Bell *et al.*

As regards accuracy of the methods, Van Kan shows that the global velocity and pressure errors in his split step scheme are of order $(\Delta t)^2$ and order Δt, respectively, and states, without proof, that the error in computing the pressure is also of order $(\Delta t)^2$. In other studies, Shen [5, 6] estimates the temporal errors in the original Chorin method, the Kim–Moin scheme [7], and other pressure splitting procedures, and finds that accuracy comparable to Van Kan's program can be obtained through use of a penalty function method. However, Shen notes that use of the penalty function procedure leads to ill-conditioned equations.

The methods given in [2–4] have an advantage over other split step schemes [6–9] and the influence matrix method [10] because they are not tightly tied to the Navier–Stokes equations, and can therefore be used to treat variable viscosity flows and two-equation turbulence models. However, if the pressure calculation is relatively inaccurate, as implied by Van Kan's error estimates and some of his calculations, the error in computing the pressure is unacceptably large when surface forces are of interest.

In the present study we remedy this defect, and we also clarify the method by showing that the approximate matrix factorization given in [4] leads immediately to the iteration procedure treated in [3] and by providing a rigorous proof that the iteration converges. The programs proposed here are derived in Section 2 and tested on a sample problem in Section 3.

2. ANALYSIS

The physical system of interest is described by the dimensionless Navier–Stokes equations,

$$\nabla \cdot \mathbf{u} = 0, \tag{1}$$

$$\frac{\partial \mathbf{u}}{\partial t} + \mathbf{u} \cdot \nabla \mathbf{u} + \nabla P = \frac{1}{\mathrm{Re}} \nabla^2 \mathbf{u} + \mathbf{f}, \tag{2}$$

where $\mathbf{u}(\mathbf{x}, t)$ and $P(\mathbf{x}, t)$ are the dimensionless velocity and pressure, $\mathbf{f}$ is a dimensionless body force, and Re is the Reynolds number. Equations (1) and (2) hold in an open spatial domain Ω with boundary $\partial\Omega$, at which some combination of $\mathbf{u}$ and its normal derivative is prescribed. In addition, the initial velocity $\mathbf{u}(\mathbf{x}, 0)$ satisfies both (1) and the boundary conditions.

* E-mail address: Stanley.Jacobs@um.cc.umich.edu.

0021-9991/95 $6.00

We begin by discretizing (1) and (2) spatially using any convenient method. The dependent variables then become u, a column vector denoting the velocity in Ω; v, a column vector denoting the velocity on $\partial\Omega$; and p, a column vector denoting the pressure, and the governing equations can be cast in the form

$$\dot{u} + c(u, v) + Gp = Ku + Lv + f, \tag{3}$$

$$Bu + Cv = g, \tag{4}$$

$$Du + Ev = 0, \tag{5}$$

$$Rp = 0, \tag{6}$$

where the vector operators in (1) and (2) are represented by matrices, denoted in (3)–(6) and below by upper case letters.

Here (3) is the discretized momentum equation, the overdot denotes a time derivative, c and Gp are the advection and pressure gradient terms, Ku and Lv represent viscous terms, and f is the body force. Equation (4) represents the boundary conditions, where g denotes a forcing term, and (5) is the discretized continuity equation. Including the velocity on the boundary as an unknown generalizes the schemes given in [2–4] and is necessary when the flow is driven by an applied stress on $\partial\Omega$.

To see the significance of (6), we note that (3) and the derivatives of (4) and (5) with respect to t provide a system of linear equations for $\dot{u}$, $\dot{v}$, and p. In general, the homogeneous version of this system admits n nontrivial pressure mode solutions $(\dot{u}, \dot{v}, p) = (0, 0, p^{(k)})$, $1 \le k \le n$, where one of the vectors $p^{(k)}$ corresponds to a spatially constant solution of $\nabla P = 0$, and the others, if any, are spurious. It follows from the Fredholm alternative theorem that the forcing terms must satisfy n solvability conditions for a solution to exist, in which case $(\dot{u}, \dot{v}, p)$ is the sum of a particular solution and a linear combination of the pressure modes. The purpose of (6) is to render the solution unique by choosing R as a matrix with the property that $Rp = 0$ projects the solution onto the orthogonal complement of the space spanned by the pressure modes. An example of the use of this procedure is given in [11].

We now discretize in time through use of the second-order backward differentiation scheme

$$\begin{aligned} \dot{u}^J &= (a_0 u^J - a_1 u^{J-1} + a_2 u^{J-2})/\Delta t, \\ c^J &= b_0 c^{J-1} - b_1 c^{J-2}, \end{aligned} \tag{7}$$

where J is a positive integer, q^J denotes the value of any dependent variable q evaluated at time $t = J\Delta t \equiv t^J$, and

$$a_0 = 1,\ a_1 = 1,\ a_2 = 0,\ b_0 = 1,\ b_1 = 0 \qquad (J = 1), \tag{8a}$$

$$a_0 = 3/2,\ a_1 = 2,\ a_2 = 1/2,$$

$$b_0 = 2,\ b_1 = 1 \qquad (J > 1). \tag{8b}$$

In this scheme the solution is advanced in time by solving the system

$$(I - \varepsilon K)u - \varepsilon Lv + \varepsilon Gp = \psi, \tag{9}$$

$$Bu + Cv = \theta, \tag{10}$$

$$Du + Ev = 0, \tag{11}$$

$$Rp = 0, \tag{12}$$

where $\varepsilon = \Delta t/a_0$, $(u, v, p) = (u^J, v^J, p^J)$, I is an appropriately dimensioned identity matrix, and ψ and θ are given by

$$\psi = (a_1 u^{J-1} - a_2 u^{J-2})/a_0 + \varepsilon(f^J - b_0 c^{J-1} + b_1 c^{J-2}), \qquad \theta = g^J. \tag{13}$$

A similar set of equations is obtained when a Crank–Nicholson/Adams–Bashforth scheme is used in place of (7).

In accord with the above discussion of the pressure modes, we assume that the enhanced system (9)–(12) is consistent and that the homogeneous equations are solved uniquely by $u = v = p = 0$. A theorem in linear algebra [12] then guarantees that (9)–(12) has a unique solution, which can be found in principle by computing the pseudo–inverse of the matrix

$$A = \begin{bmatrix} I - \varepsilon K & -\varepsilon L & \varepsilon G \\ B & C & 0 \\ D & E & 0 \\ 0 & 0 & R \end{bmatrix}. \tag{14}$$

The Uzawa strategy for inverting A consists of defining matrices U and V as the solution of

$$(I - \varepsilon K)U - \varepsilon LV = G, \qquad BU + CV = 0, \tag{15}$$

and of solving the system

$$(I - \varepsilon K)\hat{u} - \varepsilon L\hat{v} = \psi - \varepsilon G\chi, \qquad B\hat{u} + C\hat{v} = \theta, \tag{16a}$$

$$\varepsilon(DU + EV)\tilde{p} = D\hat{u} + E\hat{v}, \qquad R\tilde{p} = 0, \tag{16b}$$

$$u = \hat{u} - \varepsilon U\tilde{p}, \qquad v = \hat{v} - \varepsilon V\tilde{p}, \qquad p = \tilde{p} + \chi, \tag{16c}$$

where χ is any vector satisfying $R\chi = 0$.

To avoid this calculation, we define the column vectors

$$x = (u, v, p)^T, \qquad y = (\psi, \theta, 0, 0)^T, \tag{17}$$

so that (9)–(12) are equivalent to $Ax = y$, and we follow Dukowicz and Dvinsky by defining the matrix

$$\bar{A} = \begin{bmatrix} I - \varepsilon K & -\varepsilon L & 0 & 0 \\ B & C & 0 & 0 \\ 0 & 0 & I & 0 \\ 0 & 0 & 0 & I \end{bmatrix} \begin{bmatrix} I & 0 & \varepsilon G \\ 0 & I & \varepsilon H \\ D & E & 0 \\ 0 & 0 & R \end{bmatrix}, \tag{18}$$

where the dimensionality of the identity matrices is determined by context and where

$$H = -C^{-1}BG. \tag{19}$$

The definitions imply that $\bar{A} - A = O(\varepsilon^2)$, and therefore, since it can be shown that $\bar{A}^{-1} = O(\varepsilon^{-1})$, it follows that

$$\|\bar{A}^{-1}(\bar{A} - A)\| = O(\varepsilon), \tag{20}$$

where $\|\cdot\|$ is any matrix norm. Consequently, for sufficiently small ε a standard theorem [13] guarantees that the scheme

$$\bar{A}(x_k - x_{k-1}) = y - Ax_{k-1}, \qquad k = 1, 2, \ldots, \tag{21}$$

converges as $k \to \infty$ for arbitrary x_0. Equation (21) is a spatially discretized version of the iteration procedure suggested by Bell *et al.*

As emphasized by Van Kan, the issue of boundary conditions does not arise in this scheme. By contrast, because Bell *et al.* discretize the Navier–Stokes equations spatially after, rather than before, the temporal discretization, they need boundary conditions on the pressure to give a meaning to Poisson equations for the pressure iterates in their iteration scheme. Bell *et al.* fail to provide such conditions and therefore, except for spatial discretizations such that boundary conditions on the pressure are not needed, their convergence proof is incomplete.

When written in explicit form, (21) becomes

$$(I - \varepsilon K)\{u_k + \varepsilon G(p_k - p_{k-1})\} - \varepsilon L\{v_k + \varepsilon H(p_k - p_{k-1})\} = \psi - \varepsilon G p_{k-1}, \tag{22}$$

$$B\{u_k + \varepsilon G(p_k - p_{k-1})\} + C\{v_k + \varepsilon H(p_k - p_{k-1})\} = \theta, \tag{23}$$

$$Du_k + Ev_k = 0, \tag{24}$$

$$Rp_k = 0. \tag{25}$$

By defining $\hat{u}_k$ and $\hat{v}_k$ as the terms in curly brackets in (22)–(23) and $\hat{p}_k$ as $(p_k - p_{k-1})$, the scheme can be cast in algorithmic form, as follows:

(1) let χ denote a known vector satisfying $R\chi = 0$ and set

$$p_0 = \chi; \tag{26a}$$

(2) For $k = 1, 2, \ldots, N$, do

(a) solve

$$(I - \varepsilon K)\hat{u}_k - \varepsilon L\hat{v}_k = \psi - \varepsilon G p_{k-1}, \qquad B\hat{u}_k + C\hat{v}_k = \theta, \tag{26b}$$

for $\hat{u}_k$ and $\hat{v}_k$;

(b) solve

$$\varepsilon(DG + EH)\hat{p}_k = D\hat{u}_k + E\hat{v}_k, \qquad R\hat{p}_k = 0, \tag{26c}$$

for $\hat{p}_k$;

(c) update by setting

$$p_k = \hat{p}_k + p_{k-1}. \tag{26d}$$

The approximate solution $(\bar{u}, \bar{v}, \bar{p})$ is given at the end of the loop by

$$\bar{u} = \hat{u}_N - \varepsilon G\hat{p}_N, \bar{v} = \hat{v}_N - \varepsilon H\hat{p}_N, \bar{p} = p_N. \tag{27}$$

If only one iteration is carried out, the scheme reduces to

$$(I - \varepsilon K)\hat{u} - \varepsilon L\hat{v} = \psi - \varepsilon G\chi, \qquad B\hat{u} + C\hat{v} = \theta, \tag{28a}$$

$$\varepsilon(DG + EH)\hat{p} = D\hat{u} + E\hat{v}, \qquad R\hat{p} = 0, \tag{28b}$$

$$\bar{u} = \hat{u} - \varepsilon G\hat{p}, \qquad \bar{v} = \hat{v} - \varepsilon H\hat{p}, \qquad \bar{p} = \hat{p} + \chi, \tag{28c}$$

and is equivalent to the method proposed in [2–4] if $\chi = p^{J-1}$, the pressure at the previous time step. For this choice of χ, a rigorous estimate given in [2] shows that the global error incurred through use of (28) is $O(\varepsilon^2)$ and $O(\varepsilon)$ with respect to the velocity and pressure, respectively, and it is claimed in [2] that the global pressure error is $O(\varepsilon^2)$.

In what follows we designate the scheme (28) with $\chi = p^{J-1}$ as program P1, and more accurate algorithms as P2, P3, and P4. The reasoning behind our first improvement is that (28) provides the exact solution of (9)–(12) if $\chi = p$, and therefore a choice of χ that decreases $\|\chi - p\|$ necessarily increases the accuracy of the computation. In program P2 we improve on the choice $\chi = p^{J-1}$ by specifying χ through

$$\chi = p^{J-1} \ (J = 1), \qquad \chi = 2p^{J-1} - p^{J-2} \ (J > 1), \tag{29}$$

so that χ is obtained from the solution at previous time steps by linear extrapolation. Sample computations discussed below show that use of (29) provides significant improvements in the accuracy of the calculation.

A further increase in the accuracy of the pressure computation is attained in programs P3 and P4 by exploiting the second-order accuracy of the velocity computation in program P2 and by noting that the pressure at any time depends only on the instantaneous velocity. In program P3 we form the system of equations for $\dot{u}$, $\dot{v}$, and p discussed earlier in connection with the pressure modes, eliminate $\dot{u}$ and $\dot{v}$, and solve

$$(DG + EH)\bar{p}_c = (D - EC^{-1}B)\{K\bar{u} + L\bar{v} + f - c(\bar{u}, \bar{v})\} + EC^{-1}B\dot{g}, \qquad R\bar{p}_c = 0, \tag{30}$$

to obtain the corrected pressure $\bar{p}_c$, where $\bar{u}$ and $\bar{v}$ are computed using (28). Similarly, in program P4 we compute $\bar{u}$ and $\bar{v}$ using (28), derive a Poisson equation for $P(\mathbf{x}, t)$ with Neumann boundary conditions by taking the divergence of (2) and evaluating the normal component of (2) on $\partial\Omega$, and again denote the solution of the spatially discretized Poisson equation by $\bar{p}_c$. In both programs the velocity and pressure are actually advanced as in program P2, and the corrected pressure is calculated solely for the purpose of reporting its value. This maintains the stability of the calculation and is economical because solution of the Poisson equation for $\bar{p}_c$ is required only at time steps for which the solution is reported.

In summary, P1 is the scheme proposed in [2–4] and requires the solution of one vector Helmholtz equation and one Poisson equation per time step. Program P2 involves the same amount of calculation, but computes χ using (29), and programs P3 and P4 require the solution of one Helmholtz equation and $(1 + 1/N)$ Poisson equations per time step, where χ is given by (29) and where the solution is reported every Nth step.

We now propose a pressure splitting scheme for use when the Navier–Stokes equations are spatially discretized using a Galerkin finite element method. If the boundary $\partial\Omega$ is a stationary solid, the solution is advanced in time by solving the algebraic system

$$(M - \varepsilon K)u + \varepsilon Gp = \phi, \qquad Du = 0, Rp = 0, \tag{31}$$

where ϕ is known and where M is the mass matrix. In principle, split step methods can be applied by multiplying the first equation in (31) by M^{-1} to obtain an equation equivalent to (9), but are inefficient because the gradient operator is then represented by the full matrix $M^{-1}G$. This problem is treated in [14] using an ad hoc theory in which the discretized momentum equation is replaced by

$$(M - \varepsilon K)u + \varepsilon M M_L^{-1} Gp = \phi,$$

where the diagonal matrix M_L is a lumped mass approximation to M.

To derive a finite element split step scheme using a consistent approximation procedure, we define $\hat{u}$ and $\hat{p}$ through

$$u = \hat{u} - \varepsilon M_L^{-1} G\hat{p}, \qquad p = \hat{p} + \chi, \tag{32}$$

where $R\chi = 0$, and substitute into (31) to obtain

$$(M - \varepsilon K)\hat{u} + \{\varepsilon^2 K + \varepsilon(M_L - M)\}M_L^{-1}G\hat{p} = \phi - \varepsilon G\chi, \tag{33}$$

$$\varepsilon D M_L^{-1} G\hat{p} = D\hat{u}, \qquad R\hat{p} = 0. \tag{34}$$

Here $\hat{p} = O(\varepsilon)$ if $\chi = p^{J-1}$ or if χ is given by (29), and therefore the term involving $\hat{p}$ in (33) is $O(\varepsilon^3 + \varepsilon^2\,\delta)$ if $\|M_L - M\| = O(\delta)$, where we assume that δ is small. Neglecting this term yields a split step scheme in which u and p are given by (32) and in which $\hat{u}$ is obtained by solving

$$(M - \varepsilon K)\hat{u} = \phi - \varepsilon G\chi \tag{35}$$

and $\hat{p}$ by solving (34). Although solving an equation analogous to (30) is inefficient in this method because it requires inversion of the full matrix $DM^{-1}G$, higher order accuracy in the computation of the pressure can be obtained through the use of program P4.

3. SAMPLE CALCULATIONS

As an example, we consider 2D Stokes flow in the channel $|z| < 1$, $-\infty < x < \infty$, where $\mathbf{u}$ vanishes on $z = \pm 1$ and where all dependent variables are periodic in x. This standard test problem is treated in [9] and [10] to evaluate routines for solving the Navier–Stokes equations.

After separating variables using $F = f(z, t)\exp(i\alpha x)$, where F is any dependent variable, employing a change of variable yields the equations

$$\frac{\partial u}{\partial t} - \alpha^2 p = \frac{1}{\mathrm{Re}}\left(\frac{\partial^2 u}{\partial z^2} - \alpha^2 u\right), \tag{36}$$

$$\frac{\partial w}{\partial t} + \frac{\partial p}{\partial z} = \frac{1}{\mathrm{Re}}\left(\frac{\partial^2 w}{\partial z^2} - \alpha^2 w\right), \tag{37}$$

$$u + \frac{\partial w}{\partial z} = 0, \tag{38}$$

together with $u = w = 0$ at $z = \pm 1$. The system (36)–(38) admits eigensolutions of the form $\exp(-\sigma t)h(z)$, and in the present calculation the analytic solution corresponding to the decay constant $\sigma = 9.314/\mathrm{Re}$ for $\alpha = 1$ was taken as the initial condition.

In the first of the spatial discretizations used here, we define

$$z_I = -\cos\left\{\frac{\pi(I-1)}{M-1}\right\}, \qquad 1 \le I \le M, \tag{39}$$

as the Chebyshev–Lobato grid points, and let D_{IK} and E_{IK} denote the first and second differentiation matrices in a pseudospectral collocation approach. After discretizing in both space and time and defining T_{IK} by

$$T_{IK} = \sum_{J=2}^{M-1} D_{IJ} D_{JK}, \tag{40}$$

TABLE I

δw for Re = 1, $M = 17$, $\alpha = 1$, and $T = 0.3$, Pseudospectral BDF Version

Δt	P1	P2	P3	P4
1.00 e-2	3.0 e-3	1.0 e-4	1.0 e-4	1.0 e-4
5.00 e-3	7.3 e-4	1.0 e-5	1.0 e-5	1.0 e-5
2.50 e-3	1.8 e-4	1.1 e-6	1.1 e-6	1.1 e-6
1.25 e-3	4.4 e-5	1.3 e-7	1.3 e-7	1.3 e-7
6.25 e-4	1.1 e-5	1.6 e-8	1.6 e-9	1.6 e-8
3.13 e-4	2.7 e-6	1.9 e-9	1.9 e-9	1.9 e-9
1.56 e-4	6.9 e-7	2.4 e-10	2.4 e-10	2.4 e-10

we find that the split step equations take the form

$$\hat{u}_I - \frac{\varepsilon}{\mathrm{Re}}\left(\sum_{K=2}^{M-1} E_{IK}\hat{u}_K - \alpha^2\hat{u}_I\right\} = r_I + \alpha^2\varepsilon\chi_I$$

$$(2 \le I \le M-1), \tag{41a}$$

$$\hat{w}_I - \frac{\varepsilon}{\mathrm{Re}}\left(\sum_{K=2}^{M-1} E_{IK}\hat{w}_K - \alpha^2\hat{w}_I\right\} = s_I - \varepsilon\sum_{K=1}^{M} D_{IK}\chi_K$$

$$(2 \le I \le M-1), \tag{41b}$$

$$\varepsilon\left\{\sum_{k=1}^{M} T_{Ik}\hat{p}_K - \alpha^2\hat{p}_I\right\} = \hat{u}_I + \sum_{k=2}^{M-1} D_{Ik}\hat{w}_K$$

$$(2 \le I \le M-1), \tag{42a}$$

$$\varepsilon\sum_{k=1}^{M} T_{Ik}\hat{p}_K = \sum_{k=2}^{M-1} D_{Ik}\hat{w}_K, \qquad \varepsilon\sum_{k=1}^{M} T_{Mk}\hat{p}_K = \sum_{k=2}^{M-1} D_{Mk}\hat{w}_K, \tag{42b}$$

where (41) corresponds to (28a) and (42) to (28b). Here u_I, w_I, and p_I are the values of u, w, and p at $z = z_I$ and $t = t^j$; r_I and s_I are known vectors; and (42b) is the continuity equation evaluated at $z = \pm 1$. The velocity and pressure are given by (28c), and the extra Poisson equations in programs P3 and P4 are similar to (42).

TABLE II

δp for Re = 1, $M = 17$, $\alpha = 1$, and $T = 0.3$, Pseudospectral BDF Version

Δt	P1	P2	P3	P4
1.00 e-2	1.8 e-1	4.4 e-2	2.8 e-3	3.6 e-3
5.00 e-3	3.0 e-2	4.3 e-3	3.9 e-4	4.9 e-4
2.50 e-3	4.8 e-3	1.0 e-4	4.6 e-5	5.8 e-5
1.25 e-3	1.1 e-3	1.3 e-5	5.7 e-6	7.2 e-6
6.25 e-4	2.7 e-4	1.6 e-6	7.0 e-7	8.9 e-7
3.13 e-4	6.7 e-5	2.0 e-7	8.8 e-8	1.1 e-7
1.56 e-4	1.7 e-5	2.5 e-8	1.1 e-8	1.4 e-8

In Tables I and II we show the errors

$$\delta q = \left|\frac{q(z_K) - \bar{q}_K}{q(z_K)}\right| \tag{43}$$

incurred through use of the split step schemes at time $t = T$, where, for any dependent variable, q is the analytical solution of the temporally discretized form of (36)–(38), z_K is the grid point at which the error attains its maximum value, and $\bar{q}_k$ is the split step numerical solution at $z = z_K$. Since the error caused by the spatial discretization is negligibly small for the value of M used in the calculation, a vanishing value of δq implies that the solutions for q calculated using the backward differentiation formula and the various split step schemes coincide.

In Fig. 1 we plot $\Delta p \equiv \|p - \bar{p}\|$ as a function of Δt, where p is the analytical solution of the temporally continuous version of (36)–(38) at time $t = T$, $\bar{p}$ is the split step solution at the same time given by the BDF versions of P1 and P3, and $\|\cdot\|$ is the Euclidean norm. As can be seen, the pressure error in program P3 is about two orders of magnitude smaller than in P1. We have also fit the values of δw and δp in Tables I and II and the value of Δp in Fig. 1 with curves of the form $\alpha(\Delta t)\beta$, where α and β are constants. This shows that program P1 is second-order accurate in the computation of w and p and that program P3 is between second- and third-order accurate in the computation of both quantities. The performance of program P3 in this problem is much better than anticipated.

To demonstrate that the high accuracy of program P3 shown in Tables I and II and in Fig. 1 is independent of the time stepping scheme, we give the values of δw and δp computed using Crank–Nicholson versions of programs P1–P4 in Tables III and IV. In addition, calculations were made for a program in which χ is given by (29), two iterations of the form (26)–(27) are carried out, and solution of the second Poisson equation

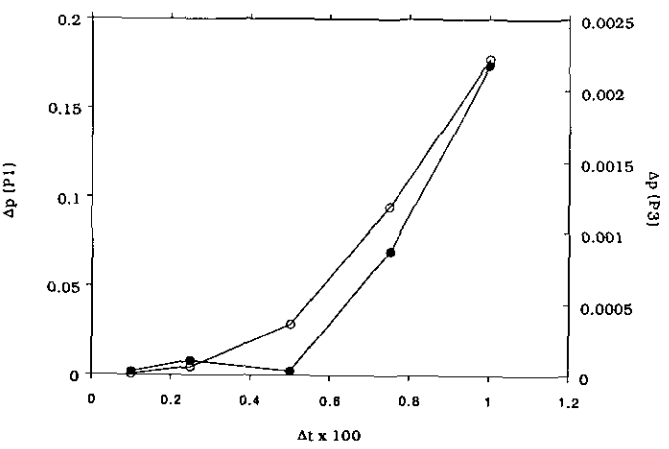

FIG. 1. Pseudospectral errors Δp for Re = 1, $M = 17$, $\alpha = 1$, and $T = 0.3$. P1 is shown by open symbols, P3 by solid symbols.

TABLE III

δw for Re = 1, M = 17, α = 1, and T = 0.3, Pseudospectral Crank–Nicholson Version

Δt	P1	P2	P3	P4
1.00 e-2	1.1 e-3	6.7 e-5	6.7 e-5	6.7 e-5
5.00 e-3	2.6 e-4	8.1 e-6	8.1 e-6	8.1 e-6
2.50 e-3	6.6 e-5	1.0 e-6	1.0 e-6	1.0 e-6
1.25 e-3	1.6 e-5	1.2 e-7	1.2 e-7	1.2 e-7

in P3 and P4 is omitted. The accuracy was found to be better than for our other programs, but not enough to compensate for the computational expense.

We now consider finite element and finite difference discretizations of (36)–(38) by defining $h = 2/(M-1)$ and by introducing the grid points

$$z_I = -1 + (I-1)h,\ 1 \le I \le M,$$
$$\bar{z}_I = z_I + h/2,\ 1 \le I \le M-1, \tag{44}$$

where u_I and w_I denote the values of u and w at $z = z_I$ and $t = t^j$, and p_I the values of p at $z = \bar{z}_I$ and $t = t^j$. Then, using piecewise linear velocity elements and piecewise constant pressure elements, the finite element equations for u_I, w_I, and p_I are $u_I = w_I = 0$ for $I = 1$ and $I = M$, and

$$(Su)_I - \frac{\varepsilon}{\mathrm{Re}}\{(Tu)_I - \alpha^2(Su)_I\} - \alpha^2\varepsilon(p_I + p_{I-1})/2 = r_I,$$
$$(2 \le I \le M-1), \tag{45}$$

$$(Sw)_I - \frac{\varepsilon}{\mathrm{Re}}\{(Tw)_I - \alpha^2(Sw)_I\} + \varepsilon(p_I + p_{I-1})/h = s_I,$$
$$(2 \le I \le M-1), \tag{46}$$

$$(u_{I+1} + u_I)/2 + (w_{I+1} - w_I)/h = 0, \qquad (1 \le I \le M-1), \tag{47}$$

where r_I and s_I are known vectors and where Sf and Tf are defined by

TABLE IV

δp for Re = 1, M = 17, α = 1, and T = 0.3, Pseudospectral Crank–Nicholson Version

Δt	P1	P2	P3	P4
1.00 e-2	5.4 e-2	4.9 e-2	1.3 e-3	1.6 e-3
5.00 e-3	7.5 e-3	1.4 e-3	1.5 e-4	1.8 e-4
2.50 e-3	1.7 e-3	3.8 e-5	1.8 e-5	2.2 e-5
1.25 e-3	4.0 e-4	4.7 e-6	2.2 e-6	2.8 e-6

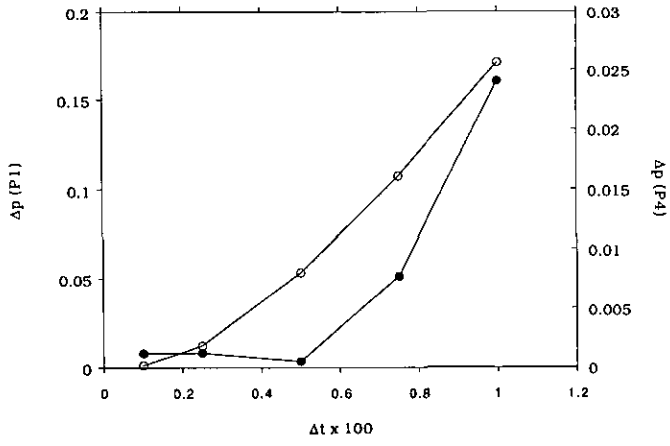

FIG. 2. Finite element errors Δp for Re = 1, M = 251, α = 1, and T = 0.3. P1 is shown by open symbols, P4 by solid symbols.

$$(Sf)_I \equiv (f_{I-1} + 4f_I + f_{I+1})/6,$$
$$(Tf)_I \equiv (f_{I-1} - 2f_I + f_{I+1})/h^2. \tag{48}$$

The corresponding finite difference equations are obtained by replacing $(Sf)_I$ by f_I. In the present finite element treatment the lumped mass matrix M_L discussed earlier is taken as the identity matrix, and programming the various split step algorithms is straightforward.

In Figs. 2 and 3 we show the program P1 and P4 pressure errors Δp for the finite difference and finite element discretizations. Since the extra Poisson equations in both versions of program P4 were solved using the same centered finite difference scheme, the poor accuracy of the finite element calculation for small Δt is necessarily due to errors caused by the lumped mass approximation, which are dominant at small step sizes. For larger step sizes use of this approximation induces no appreciable loss of accuracy in the present problem. As regards order of accuracy,

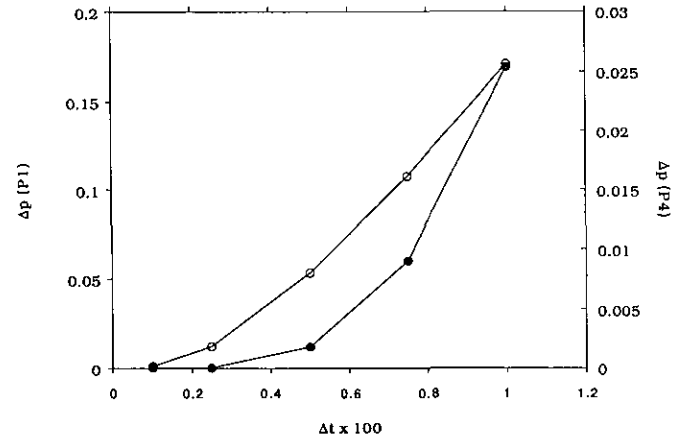

FIG. 3. Finite difference errors Δp for Re = 1, M = 251, α = 1, and T = 0.3. P1 is shown by open symbols, P4 by solid symbols.

curve fitting suggests that calculation of the pressure is second order accurate for all computations shown in the figure, but that programs P3 and P4 yield smaller errors than P1.

As a final example, we consider the driven cavity problem. In our version of the problem, this consists of computing two-dimensional flow in the rectangle $a \le x \le b$, $c \le y \le d$, with initial conditions $u = v = p = 0$, and with boundary conditions

$$\begin{aligned} &u = 0 \text{ at } x = a \text{ and } x = b, \qquad u = B(x) \text{ at } y = c, \\ &\qquad\qquad u = T(x) \text{ at } y = d, \\ &v = 0 \text{ at } y = c \text{ and } y = d, \qquad v = L(y) \text{ at } x = a, \\ &\qquad\qquad v = R(y) \text{ at } x = b, \end{aligned} \tag{49}$$

where B, T, L, and R are prescribed.

To treat this problem we introduce the grid points $x_I = a + I\,\Delta x$, $y_J = c + J\,\Delta y$, where $\Delta x = (b - a)/M$, $\Delta y = (d - c)/N$, $0 \le I \le M$, and $0 \le J \le N$, and we suppress a possible checker board pressure oscillation by defining the discretized velocity components $(u_{I,J}, v_{I,J})$ and the discretized pressure $p_{I,J}$ by

$$\begin{aligned} u_{I,J} &= u(x_I, y_{J-1/2}, t),\ v_{I,J} = v(x_{I-1/2}, y_J, t), \\ p_{I,J} &= p(x_{I-1/2}, y_{J-1/2}, t), \end{aligned} \tag{50}$$

where $u_{I,J}$ is defined for $0 \le I \le M$, $1 \le J \le N$; $v_{I,J}$ for $1 \le I \le M$, $0 \le J \le N$; and $p_{I,J}$ for $1 \le I \le M$, $1 \le J \le N$. As in other computations using finite differences on a staggered grid, we evaluate the continuity equation, the x momentum equation, and the y momentum equation at the pressure grid points, the u grid points, and the v grid points, respectively, using centered difference formulae to approximate spatial derivatives. In this method the velocity component v evaluated at a u grid point in the x momentum equation and the velocity component u evaluated at a v grid point in the y momentum equation are approximated as averages of their four nearest neighbors. Values of u in the x momentum equation and of v in the y momentum equation evaluated at points outside the flow domain are determined here using quadratic extrapolation.

We now discretize the equations temporally and define U, V, and P as the matrices with components $u_{I,J}$, $v_{I,J}$, and $p_{I,J}$ at time step t^J. Then, incorporating the boundary conditions into the governing equations and recalling the definition of ε following (12), the discretized continuity and momentum equations take the form

$$AU + BV = 0, \tag{51}$$

$$U - \frac{\varepsilon}{\mathrm{Re}}(EU + UF^T) + \varepsilon CP = X, \tag{52}$$

$$V - \frac{\varepsilon}{\mathrm{Re}}(GU + VH^T) + \varepsilon PD^T = Y, \tag{53}$$

where A, ..., H are matrices representing differentiation, the superscript T denotes the transpose, the matrices X and Y are known at time t^J, and U, V, and P are defined on the interior grid points. An arbitrary additive scalar constant in the solution for P is determined here by requiring that

$$\sum_{I=1}^{M}\sum_{J=1}^{N} p_{I,J} = 0. \tag{54}$$

In the basic split step scheme, we let Q denote a known close approximation to P, express U, V, and P in the form

$$U = \hat{U} - \varepsilon C\hat{P}, \qquad V = \hat{V} - \varepsilon \hat{P}D^T, \qquad P = \hat{P} + Q, \tag{55}$$

and approximate the governing equations as in (28). This yields the uncoupled Helmholtz equations

$$\hat{U} - \frac{\varepsilon}{\mathrm{Re}}(E\hat{U} + \hat{U}F^T) = X - \varepsilon CQ, \tag{56}$$

$$\hat{V} - \frac{\varepsilon}{\mathrm{Re}}(G\hat{V} + \hat{V}H^T) = Y - \varepsilon QD^T, \tag{57}$$

and the Poisson equation

$$\varepsilon\{(AC)\hat{P} + \hat{P}(BD)^T\} = A\hat{U} + \hat{V}B^T. \tag{58}$$

In the present study, (56) and (57) were solved using the V cycle multigrid algorithm described by Hackbusch on p. 33 of [15], with semicoarsening and line Gauss–Seidel iteration used as the smoothing operations. The prolongation and restriction operators employed in the calculation are based on a combination of linear interpolation and linear extrapolation. These procedures, together with a multigrid algorithm for treating singular systems given on p. 266 of [15], were used to solve (58) subject to (54) and to solve (54) and the equation corresponding to (30). In contrast to Van Kan's experience, no problems were incurred in the calculation of the pressure.

Computations for various combinations of Reynolds number, grid spacing, and temporal step size were carried out for the regularized driven cavity problem described by $a = c = 0$, $b = d = 1$, and by $B(x) = L(y) = R(y) = 0$, $T(x) = 16x^2(1 - x)^2$. For the moderate Reynolds number case $\mathrm{Re} = 100$, a close approximation to the exact solution of the spatially discretized equations was computed by integrating using a step size $\Delta t = 1.25 \times 10^{-3}$. This solution was used to compute the errors δu and δp shown in Tables V and VI. As can be seen, in this computation the error δp computed using P1 is small, and no real advantage is obtained by using program P3.

Computations were also made for a larger Reynolds number, $\mathrm{Re} = 5000$, using a 64×64 grid. In treating this problem, we computed the ratio

$$K(\Delta t, t, q) = \frac{|q(\Delta t, t) - q(\Delta t/2, t)|}{|q(\Delta t/2, t) - q(\Delta t/4, t)|}, \tag{59}$$

TABLE V

δu for Re = 100, $M = N = 16$, and $T = 1$, BDF Solution of Driven Cavity Problem

Δt	P1	P3
0.2	1.9 e-2	3.6 e-2
0.1	3.2 e-3	2.4 e-2
0.05	6.6 e-4	5.6 e-4
0.025	1.6 e-4	1.4 e-4
0.01	2.8 e-5	2.6 e-5

where $q(\Delta t, t)$ is the numerical solution at time t for any variable q computed using a time step Δt, and $|\cdot|$ is the maximum modulus norm. This ratio should equal 4 for a second order scheme. Computations for both the large Reynolds number case and for the case summarized in Tables V and VI showed values of $K(0.05, 1, q)$ for $q = (u, v, p)$ varying between 3.7 and 4.6 for programs P1, P2, and P3. On the basis of this relatively limited computational experience, it appears that all three schemes are second-order accurate when applied to the version of the driven cavity program treated here.

4. DISCUSSION

In early versions of programs P3 and P4 the equations for $\bar{p}_c$ were solved at all time steps and the solution was advanced in time by taking $p = \bar{p}_c$ at time t', as suggested on pp. 596–599 of [8]. When applied to the sample problem treated above, this procedure provided good accuracy for small step sizes but was otherwise disastrous because of numerical instability. Consequently, if an extra Poisson equation is solved to improve the accuracy of the computed pressure, as in the programs in [8] discussed above and in our P3 and P4, we suggest advancing the solution in time using the basic split step scheme and calculating the corrected pressures $\bar{p}_c$ only for the purpose of reporting their values.

The results of the sample calculations and Van Kan's analysis imply that all our programs provide a second order accurate solution for the velocity, and the computational evidence accumulated here supports Van Kan's claim that the pressure calculation in scheme P1 is also second order accurate. Accordingly, it appears that second-order accuracy in the computation of the velocity and pressure can be obtained by solving one vector Helmholtz equation and one Poisson equation per time step, (28a) and (28b) or (35) and (34) above.

TABLE VI

δp for Re = 100, $M = N = 16$, and $T = 1$, BDF Solution of Driven Cavity Problem

Δt	P1	P3
0.2	7.4 e-2	9.3 e-2
0.1	3.1 e-3	1.8 e-3
0.05	6.8 e-4	5.2 e-4
0.025	1.5 e-4	1.4 e-4
0.01	2.7 e-5	3.2 e-5

In addition, our computational results suggest that the error in computing the pressure can be reduced in most of our examples by solving an additional Poisson equation, for example (30) in program P3. This is admittedly vague, and a rigorous estimate of the error in computing the pressure would be desirable. In particular, it would be useful to determine if the rather poor accuracy for the pressure often obtained in split step schemes is intrinsic to the splitting procedure or is caused by an inappropriate spatial discretization.

We conclude by noting that the type of spatial discretization affects the accuracy of the computation because all split step methods are based on the assumption that the discretized version of the operator $\Delta t(\nabla^2)$ is small. In particular, in the pseudospectral example treated here the use of excessive spatial resolution in the calculation leads to a loss of accuracy because the matrix K then has a large norm, thus invalidating the approximation of (16) by (28).

ACKNOWLEDGMENTS

This work was sponsored under the Program in Ocean Surface Processes and Remote Sensing at the University of Michigan, funded under the University Research Initiative of the Office of Naval Research, Contract N00014-92-J1650.

REFERENCES

1. A. J. Chorin, *Math. Comput.* **22,** 745 (1968).
2. J. Van Kan, *SIAM J. Sci. Stat. Comput.* **7,** 870 (1986).
3. J. B. Bell, P. Coelella, and H. M. Glaz, *J. Comput. Phys.* **85,** 257 (1989).
4. J. K. Dukowicz and A. S. Dvinsky, *J. Comput. Phys.* **102,** 336 (1992).
5. J. Shen, *SIAM J. Numer. Anal.* **29,** 57 (1992).
6. J. Shen, *Numer. Math.* **62,** 49 (1992).
7. J. Kim and P. Moin, *J. Comput. Phys.* **59,** 308 (1992).
8. P. M. Gresho, *Int. J. Numer. Methods Fluids* **11,** 587 (1990).
9. G. E. Karniadakis, M. Israeli, and S. A. Orszag, *J. Comput. Phys.* **97,** 414 (1991).
10. M. Deville, L. Kleiser, and F. Montigny-Rannous, *Int. J. Numer. Methods Fluids* **4,** 1149 (1984).
11. A. Farcy and T. Aliziary de Roquefort, *Comput. Methods Appl. Mech. Engg.* **80,** 337 (1990).
12. P. Lancaster and M. Tismenetsky, *The Theory of Matrices,* 2nd ed. (Academic Press, San Diego, 1985), p. 424.
13. E. Isaacson and H. B. Keller, *Analysis of Numerical Methods* (Wiley, New York, 1966), p. 62.
14. P. M. Gresho and S. T. Chan, *Int. J. Numer. Methods Fluids* **11,** 621 (1990).
15. W. Hackbusch, *Multi-grid Methods and Applications* (Springer-Verlag, New York, 1985).